Journal of Materials and Engineering Structures

Research Paper

Modeling of Internally or externally prestressed concrete beams until fracture in nonlinear elasticity

Iddir Abdelkader [a*], *Youcef Bouafia* [a], *Mohand Said Kachi* [a], *Hélène Dumontet* [b], *Salma Barboura* [c]

[a] *Civil Engineering departement, Mouloud Mammeri University, 15000, Tizi-Ouzou, Algeria*

[b] *Jean Le Rond d'Alembert Institut, Paris 6 University , C.N.R.S. U.M.R.7190, BP 161, Paris, France*

[c] *C.N.R.S. LSPM-UPR3407 Laboratory, Paris 13 University, Paris, France*

ARTICLE INFO

Article history :

Received : 10 April 2021

Revised : 12 March 2022

Accepted : 25 March 2022

Keywords:

Non linear elasticity

Modeling ; External prestress

Shear modulus

Slipping of the tendon

ABSTRACT

In this paper, we present an analytical model to analyze reinforced and prestressed concrete beams loaded in combined bending, axial load and shear, in the frame of non linear elasticity. In this model, the equilibrium of the beam is expressed by solving a system of equations, governing beams equilibrium, based on the stiffness matrix of the beam, which connects the load vector to the node displacements vector of the beam. It is built from the stiffness matrix of the section which takes into account a variation of the shearing modulus (depending on the shear variation) instead of assuming a constant shearing modulus as in linear elasticity. For the internal tendons, the stiffness matrix is completed by the terms due to the prestress effect in flexural equilibrium and by the balancing of one part of the shear by the transverse component of the force in the inclined cables. A computing method is then developed and applied to the calculus of some internally or externally prestressed concrete beams. The comparison of the results predicted by the model with several experimental results show that, on the one hand, the model predictions give a good agreement with the experimental behavior in any field of the behavior (after cracking, post cracking, post steel yielding and fracture of the beam); and, on the second hand, that the model leads to the prediction of tendons slipping at deviators and to the tension increase in the tendons.

1 Modelling

1.1 Geometrical and cinematically hypothesis

The structure studied is a reinforced concrete beams or prestressed beams with internal or external tendons. In this last case, the tendons are relied to the concrete only at the deviators who considered as rigid elements [1-11]. The concrete beam is divided into beams elements and for the externally prestressed beams, the external cable is divided into cable elements to obtain the model for the analysis (figure 1).

* *Corresponding author. Tel.: +213.(0)560.02.55.42..*
E-mail address: abdelkader.iddir@ummto.dz

e-ISSN: 2170-127X,

RESEARCH REVIEW of Sciences and Technologies

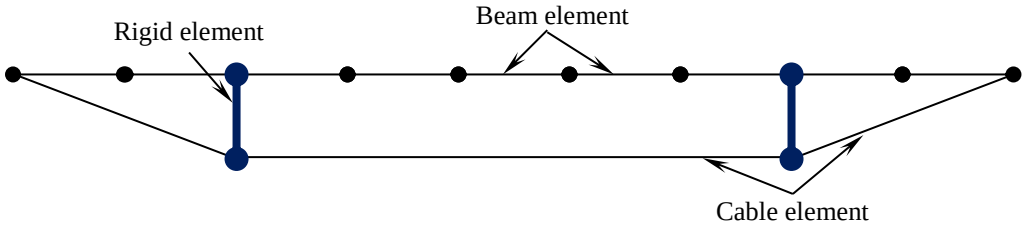

Fig. 1 - Schematic model of the externally prestressed beam for the analysis.

The transverse section of the beam is decomposed into layers (see figure 2). The deformation of the section follows Bernoulli's principle.

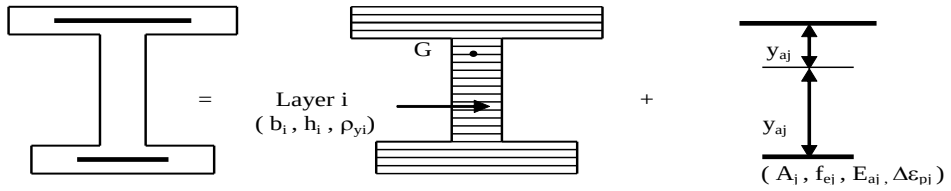

Fig. 2 – Section discretised into concrete strips and longitudinal steel components.

The following systems of axes are introduced to study the equilibrium of an element: a fixed global system attached to the structure; a local system concerning the initial position of the element; an intrinsic system linked to the deformed position of the element; and an intermediate system related to the translation of the local system to the origin of the intrinsic system (see figure 3).

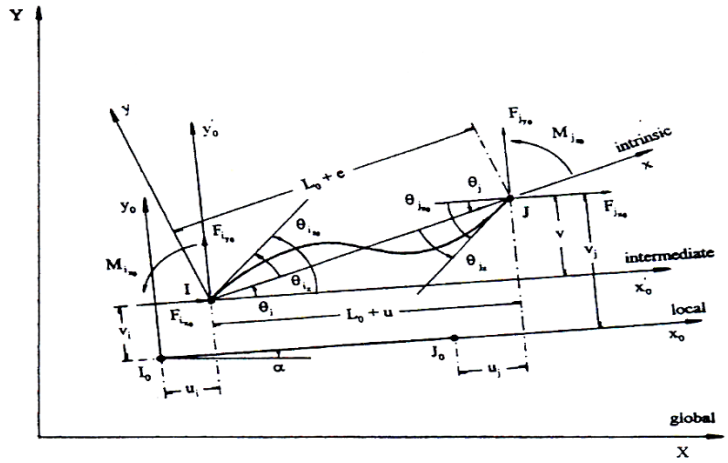

Fig. 3 - Axis of the beam element.

The evaluation of the displacement field of the elements is made by numerical integration of deformations section by section. The deformations of a section are calculated by use of the intrinsic system. It is assumed that deformation and displacements are small. The second order effects due to node displacements are introduced by a non linear transformation of displacements at element ends from the intrinsic system to the intermediate system [8, 12-14].

1.2 Constitutive laws of materials

1.2.1 Concrete constitutive law

Many mechanical models of compressive concrete are currently used in the analysis of reinforced or prestressed concrete structures. Among those models, the monotonic curve introduced by Sargin [15] was adopted in this study for its simplicity and computational efficiency. In this model the stress strain relationship is:

$$\sigma = f_{cj}\frac{k_b\bar{\varepsilon}-(k_b^{'}-1).\bar{\varepsilon}^2}{1+(k_b-2)\bar{\varepsilon}-k_b^{'}\bar{\varepsilon}^2} \tag{1}$$

where $\bar{\varepsilon}=\dfrac{\varepsilon}{\varepsilon_0}$ and $k_b=\dfrac{E_{c0}.\varepsilon_0}{f_{cj}}$

For a normal concrete, it generally takes $k_b^{'}=k_b-1$ [15].

On the other hand, we assume that concrete is linearly elastic in the tension region. Beyond the tensile strength, the tensile stress decrease with increasing the tensile strain. In this field we have adopted the monotonic concrete stress-strain curve introduced by Grelat [5] for describe this decreasing branch. Ultimate failure is assumed to take place by cracking, when the tensile strains exceed the yielding strain of the reinforcement. In this model monotonic concrete tensile behavior is described by formulas (2) where tensile strain is considered negative:

$$\begin{cases}\sigma = E_{c0}.\varepsilon & \text{where} \quad |\varepsilon|<\varepsilon_{ct}\\ \sigma_t = -f_{ct}\dfrac{(\varepsilon-\varepsilon_{rt})^2}{(\varepsilon_{rt}-\varepsilon_{ct})^2} & \text{where} \quad |\varepsilon_{ct}|<\varepsilon<|\varepsilon_{rt}|\\ \sigma_t = 0 & \text{where} \quad \varepsilon>|\varepsilon_{rt}|\end{cases} \tag{2}$$

1.2.2 Reinforcement constitutive law

Reinforcing steel is modeled as linear elastic, with yield stress σ_e, as:

$$\begin{cases}\sigma = E_a.\varepsilon & \text{where} \quad \varepsilon<\varepsilon_e\\ \sigma=\sigma_e & \text{where} \quad \varepsilon_e<\varepsilon<\varepsilon_u\\ \sigma=0 & \text{where} \quad \varepsilon>\varepsilon_u\end{cases} \tag{3}$$

1.2.3 Prestress constitutive law

Behaviour of prestressing steels is represented by the law recommended by regulation BPEL91 [15].

$$\begin{cases}\sigma_p = E_p.\varepsilon_p & 0<\sigma<0.9\sigma_{ep}\\ \varepsilon_p=\dfrac{\sigma_p}{E_p}+100\left(\dfrac{\sigma_p}{f_{ep}}-0.9\right)^5 & 0.9\sigma_{ep}<\sigma<1.06\sigma_e\\ \varepsilon_p=1.06\sigma_{ep} & \varepsilon_p>2\%\end{cases} \tag{4}$$

1.3 Equilibrium of the beam element

The beams elements and the external cable elements have both 6 degrees of freedom. The cable elements have no response to compressive loads. Elements are decomposed into intermediate sections in order to evaluate the non linear behavior of concrete and reinforcement (bars and bonded internal cables). The normal deformation of a section is given by $\varepsilon(y)=\delta u+\delta w.y$ and its transverse deformation (or distortion) is defined by γ_{moy}. The contribution of this deformation is taken into account by a non linear approach. In the case of an internal prestressed tendon it is necessary to take into account the "predeformation" in the cable. This predeformation represents the difference between the deformation of the tendon and that of the concrete at the same level, at the initial tensioning.

The deformation increase vector of the section is given by (Eq.5):

$$\Delta\overset{\mathrm{r}}{\delta} = \left\{\Delta\delta u \quad \Delta\delta w \quad \Delta\gamma_{moy}\right\}^T \tag{5}$$

The equilibrium equation of the section in the intrinsic system is given by:

$$\Delta \underset{\sim}{F}_S + \Delta \underset{\sim}{P}_S = K_S \Delta \underset{\sim}{\delta} \tag{6}$$

This equation is solved by an iterative method. Its solution may be written as (Eq.7):

$$\Delta \underset{\sim}{\delta} = K_S^{-1} \left\{ \Delta \underset{\sim}{F}_S + \Delta \underset{\sim}{P}_S \right\} \tag{7}$$

Loads acting over the section are functions of the applied forces at element nodes. Their expression is given by (Eq.8):

$$\Delta \underset{\sim}{F}_S = \left[L(x) \right] . \Delta \underset{\sim}{F}_n \quad \text{with} \quad \left[L(x) \right] = \begin{bmatrix} -1 & 0 & 0 \\ 0 & -(1-x/L) & x/L \\ 0 & 1/L & 1/L \end{bmatrix} \tag{8}$$

If the length variation of the element is neglected, the expression of the deformation vector $\Delta \underset{\sim}{S}_n$ of the beam element, in the intrinsic system, is given using the virtual work theorem which stipulates that the virtual work of the section's deformations increase is equal to the virtual work of the section's loads increase, by (Eq.9):

$$\Delta \underset{\sim}{S}_n = \int_0^L L^T(x) \Delta \underset{\sim}{\delta}(x)\, dx \tag{9}$$

Thus, we may write the equilibrium equation of the element in the intrinsic system as follows:

$$\Delta \underset{\sim}{F}_n + \Delta \underset{\sim}{P}_n = K_n \Delta \underset{\sim}{S}_n \tag{10}$$

the stiffness matrix K_n of the element evaluated as follows:

$$K_n^{-1} = \int_0^L L^T(x) K_S^{-1} L(x)\, dx \tag{11}$$

The second order effects are introduced by transforming the equation from intrinsic system to intermediate system. In fact, the relationship between the expressions of the displacement in intrinsic and intermediate systems is given by (Eq.13):

$$\Delta \underset{\sim}{S}_n = B \Delta \underset{\sim}{S}_u \tag{12}$$

where

$$B = \begin{bmatrix} e_{,u} & e_{,v} & 0 & 0 \\ -\theta_{,u} & -\theta_{,v} & 1 & 0 \\ -\theta_{,u} & -\theta_{,v} & 0 & 1 \end{bmatrix} \text{ and } \quad e_{,u} = \frac{\partial e}{\partial u}$$

The equilibrium equation in the intermediate system is given as follows by (Eq. 13):

$$\Delta \underset{\sim}{F}_u + \Delta \underset{\sim}{P}_u = \left(B^T K_n B + D \right) \Delta \underset{\sim}{S}_u \tag{13}$$

where

$$D = \begin{bmatrix} d & 0 \\ 0 & 0 \end{bmatrix} \text{ and } \quad d = \frac{1}{L_0^2} \begin{bmatrix} 2vF_{j_{y0}} & -F_{j_{y0}} L_0 \\ -F_{j_{y0}} L_0 & F_{j_{x0}} L_0 - v\, F_{j_{y0}} \end{bmatrix} \tag{14}$$

The matrix d is calculated by neglecting the displacement contribution due to u and the non-linear term due to v and the null matrix is denoted by 0.

In the local system, using transformation matrix T_0, the element equilibrium may be written as:

$$\Delta\dot{F}_L + \Delta\dot{P}_L = T_0^T \left(BK_nB + D\right)T_0 \ \Delta\dot{S}_L \tag{15}$$

The element stiffness matrix in the local system may finally be written as (Eq.16):

$$K_L = T_0^T \left(BK_nB + D\right)T_0 \tag{16}$$

Using the rotation matrix T_G, the equilibrium equation on the global system may be written as:

$$\Delta\dot{F}_G + \Delta\dot{P}_G = T_G^T K_L T_G \Delta\dot{S}_G = K_G \Delta\dot{S}_G \tag{17}$$

1.4 Stiffness matrix of the transverse section

The expression of the stiffness matrix $\left[K_s\right]$ of the section is then written as (Eq.18):

$$\left[K_s\right] = \begin{bmatrix} \dfrac{\Delta N}{\Delta\delta u} & \dfrac{\Delta N}{\Delta\delta w} & 0 \\ \dfrac{\Delta M}{\Delta\delta u} & \dfrac{\Delta M}{\Delta\delta w} & 0 \\ 0 & 0 & \dfrac{\Delta V}{\Delta\gamma_{moy}} \end{bmatrix} \tag{18}$$

In the expression adopted for $\left[K_s\right]$ the shearing modulus $G = f\left(E\right)$ is not assumed to be constant as in linear elasticity but is taken as a function of the shear variation. Indeed, the coupling terms between ΔN and $\Delta\delta w$ and those between ΔM and $\Delta\delta u$ cannot be ignored in flexural analysis. But we assume that the coupling terms between ΔN and $\Delta\gamma_{moy}$ (or ΔV and $\Delta\delta u$), and between ΔM and $\Delta\gamma_{moy}$ (or ΔV and $\Delta\delta w$), are negligible. The couplings mentioned in the introduction between the strength due to V and those due to $\left(N, M\right)$ may be taken into account by the dependence of $\Delta\gamma_{moy}$ on stresses and strains due to N and M. For the prestressed beams, the matrix $\left[K_s\right]$ is completed by the terms due to the prestress effect in flexural equilibrium and by a balancing of one part of shear by the transverse component of the force in the inclined cables [5, 16]. The flexural terms ($\Delta N/\Delta\delta u, \Delta N/\Delta\delta w, \Delta M/\Delta\delta u$ and $\Delta M/\Delta\delta w$) are evaluated by classical methods. For the evaluation of the shear terms $\left(\Delta V/\Delta\gamma_{moy}\right)$, a method is proposed. In this way, the problem is reduced to the evaluation of the middle distortion γ_{moy} of transverse sections submitted to combined bending moment, normal load and shear. In this field, using the virtual work theorem, we use the equality of the external shear work to the internal shear work evaluated in each layer:

$$\Delta w_e = \sum_1^m \Delta w_i \tag{19}$$

The expression of the external shear work and of internal shear evaluated in each layer, which may be written as:

$$\Delta W_e = \Delta V.\Delta\gamma_{moy} \quad \text{and} \quad \Delta W_i = b_i.h_i.\Delta\tau_i.\Delta\gamma_i \tag{20}$$

Finally, the mean distortion of the section is given by (Eq.21):

$$\Delta\gamma_{moy} = \sum_{1}^{m} \frac{\Delta\tau_i \; b_i \; h_i \; \Delta\gamma_i}{\Delta V} \tag{21}$$

where $\Delta\gamma_i$ is the shear stress increase evaluated at the layer i. It is determined by analysing for each section S_1 of the beam loaded by an axial load N_1, bending moment M_1 and shear V_1, a second section S_2 of the beam, loaded by ($N_2 = N_1$, $M_2 = M_1 - sV_1$, $V_2 = V_1$), located at a small distance s from the first. Both sections are analyzed for the same shear stress distribution, satisfying sectional equilibrium in each case. The value of the shear stress in the layer i is obtained by solving the free-body equilibrium of the layer i between the two sections. The local distortion increase $\Delta\gamma_i$ is determined at each layer by solving a complex system of equations, namely equilibrium equations, compatibility equations and constitutive laws of the materials. It is worth to note that one uses an iterative technique to find the angle of inclination of the diagonal compression based on stress and strain Mohr's circles properties. A more detailed description of the solution procedure for the determination of these parameters may be found in Kachi & *al.* [7].

1.5 External prestress-cable element

The length of a cable element is defined between two successive deviators (see figure 1). Cables elements are beams elements with only tensile efforts. These elements are linked to others beams elements by means of rigid elements. In the external tendon the strain is a function of the whole structure deformation and the predeformation is no longer defined in relation with the strain in the section (as in an internal tendon) but in relation with the variation of length of the element.

Similarly, to beams element, the deformation increase vector of the section is given by:

$$\Delta\underline{\underline{\delta}} = \left\{\Delta\varepsilon_g \quad 0 \quad 0\right\}^T \tag{22}$$

The equilibrium equation of the section in the intrinsic system is given by:

$$\Delta\underline{\underline{F_S}} + \Delta\underline{\underline{P}} = K_{SC}\,\Delta\underline{\underline{\delta}} \tag{23}$$

the stiffness matrix $\left[K_{SC}\right]$ of the section of the cable element, is given by:

$$\left[K_{SC}\right] = Ep\;Ap \begin{bmatrix} 1 & 0 & 0 \\ 0 & 0 & 0 \\ 0 & 0 & 0 \end{bmatrix}$$

The solution of this equation is obtained iteratively as (Eq.24):

$$\Delta\underline{\underline{\delta}} = K_{SC}^{-1}\left\{\Delta\underline{\underline{F_S}} + \Delta\underline{\underline{P_S}}\right\} \tag{24}$$

In the same way, the relation whose link the displacements on intrinsic system and intermediate system and the displacements on intermediate system and local system and the displacements on local system and global system established for the beams element can be used for the cable element.

The assembly of all elementary matrices into the global system leads to the following expression of the equilibrium equation of the structure:

$$\Delta\underline{Q} + \Delta\underline{P} = R\,\Delta\underline{U} \tag{25}$$

1.6 Modelization of the slipping of the external tendons at the deviators

Generally, the behaviour of the external tendons presents, under a little level of loading, a linear phase, but gradually, when the loads increase, it becomes both non linear and non reversible. Thus, cables may slip at deviators. Equilibrium of

the structure is first expressed by assuming that no slip has occurred at deviators at each stage of the external loads. After doing so, we have to verify, for each deviator, whether or not the following inequalities are respected:

$$F_{d-1}^{j} e^{-(f_i \Delta\theta_d + \phi.L_d)} - A_d \leq F_d^j \leq F_{d-1}^{j} e^{(f_i \Delta\theta_d + \phi.L_d)} + A_d \tag{26}$$

The expression of A_d in the deviator k is developed and more details are given in [6], it may be written as follows:

$$A_d = \frac{\tau_u \ \phi_e \ \pi r}{\varphi_{eq}} (1 - e^{-\varphi_{eq} \Delta\theta_d}) ; \quad \varphi_{eq} = (f.\Delta\theta_k + \varphi.L_k) / \Delta\theta_k \tag{27}$$

We denote by $\Delta\theta_k$ the difference $|\theta_{d-1} - \theta_d|$.

If the inequalities are satisfied at each deviator, then there is no slipping; if not, the cable has slipped and, as a consequence, the tension in the cable element varies. Thus, an iterative procedure is necessary to bring the equilibrium of the structure to a successful conclusion.

In this case we note $(\beta_d g_d)$ the slipping at the deviator k, and β_d determines the sense of the slipping (if $\beta_d = 1$, the slipping is from left to right; if $\beta_d = -1$ the slipping is from right to left; and if $\beta_d = 0$ there is no slipping). Thus, the slipping is such as the following equations are verified:

$$F_{d-1}^{*} = F_d^{*} \ e^{-\phi_{d-1} \ \phi_{eq} \ \Delta\theta_k} - \beta_{d-1} A_d \quad \text{with} \quad \begin{cases} F_{d-1}^{*} = F_{d-1}^{(j)} + \Delta F_{d-1}^{(j)} \\ F_d^{*} = F_d^{(j)} + \Delta F_d^{(j)} \end{cases} \tag{28}$$

The slipping may happen at several deviators, either at the same time or consecutively. The interaction between efforts within cable elements must be taken into account, because the direction of slipping may be different. The variation of length of the cable element going from deviator $(d-1)$ to the deviator (d) is given by:

$$\Delta L_d = \beta_d g_d - \beta_{d-1} g_{d-1} \tag{29}$$

In the general case where we have several simultaneous slipping, the equation connecting slipping to the tension in the cable elements may be written as follows:

$$G \ \Delta \underline{\underline{g}} = \underline{\underline{F}}_k \tag{30}$$

The expression of the rigidity matrix of slipping G is

$$G = \begin{bmatrix} G_{11} & G_{12} & G_{13} & 0 & 0 & 0 & 0 & 0 \\ G_{21} & G_{22} & G_{23} & 0 & 0 & 0 & 0 & 0 \\ 0 & G_{32} & G_{33} & G_{34} & 0 & 0 & 0 & 0 \\ 0 & 0 & 0 & 0 & 0 & 0 & 0 & 0 \\ 0 & 0 & 0 & 0 & 0 & G_{n-1\,n-2} & G_{n-1\,n-1} & G_{n-1\,n} \\ 0 & 0 & 0 & 0 & 0 & 0 & G_{n\,n-1} & G_{n\,n} \end{bmatrix} \tag{31}$$

where $G_{ii} = \beta_i \frac{E_i}{L_i} Ap - \beta_i \frac{E_{i+1}}{L_{i+1}} Ap \ \lambda_i$; $G_{ii+1} = \beta_{i+1} \frac{E_{i+1}}{L_{i+1}} Ap \ \lambda_i$; $G_{ii-1} = \beta_{i-1} \frac{E_i}{L_i} Ap$; $F_{kn} = F_n - F_{n+1} \lambda_n + \beta_n Ad_n$

with $\lambda_i = e^{-\beta_i \ \phi_{eqi} \ Ld}$

At a stage *j* of loading, when a slipping is detected in former verifications, iterative procedures are again performed to solve this system of equations to determine the values of the slipping. We may thus evaluate the variation of the tension in the cable elements and obtain a new balanced structural state applied at the deviators to take into account the chronological emergence of slipping at the different deviators, at each stage of external loading.

2 Procedure of the calculation

A step-by-step procedure is adopted to simulate the applied monotonic loading at each stage; iterative loops are completed until reaching force balance state. During this iterative procedure for equilibrium of external loads the slipping of external tendon at the deviators are considered as negligible.

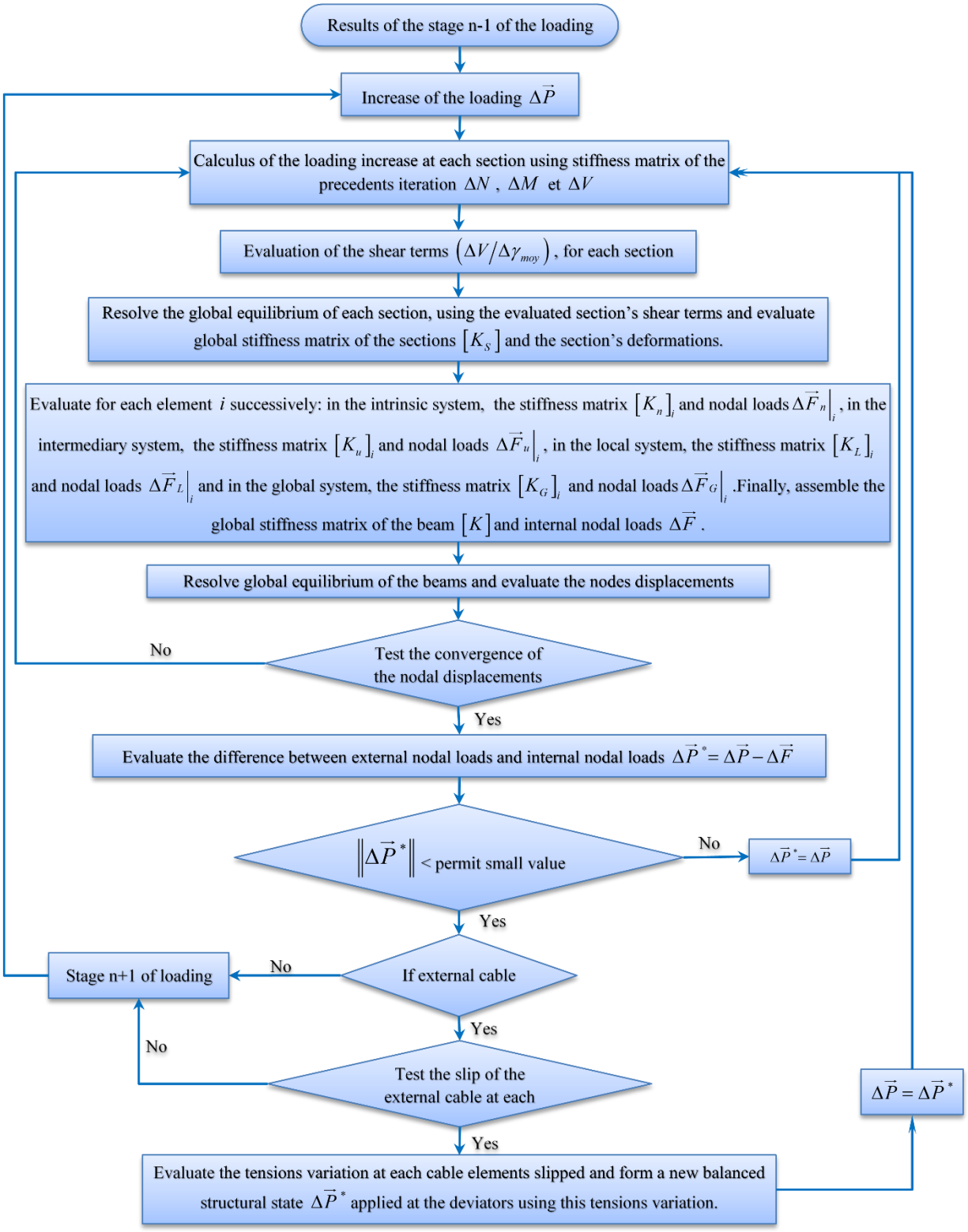

Fig.4 – Calculation steps.

After each stage of equilibrium of the structure, we verify, at each deviator, whether the slipping condition is satisfied or not. If this condition is verified at each deviator, there is no slipping at the deviators and the calculated solution is considered as correct. Otherwise the cable has slipped and an iterative procedure is then adopted to calculate the complete equilibrium of the structure. The procedure of the calculation for the stage n of the beams loading is presented in Fig. 4 and 5.

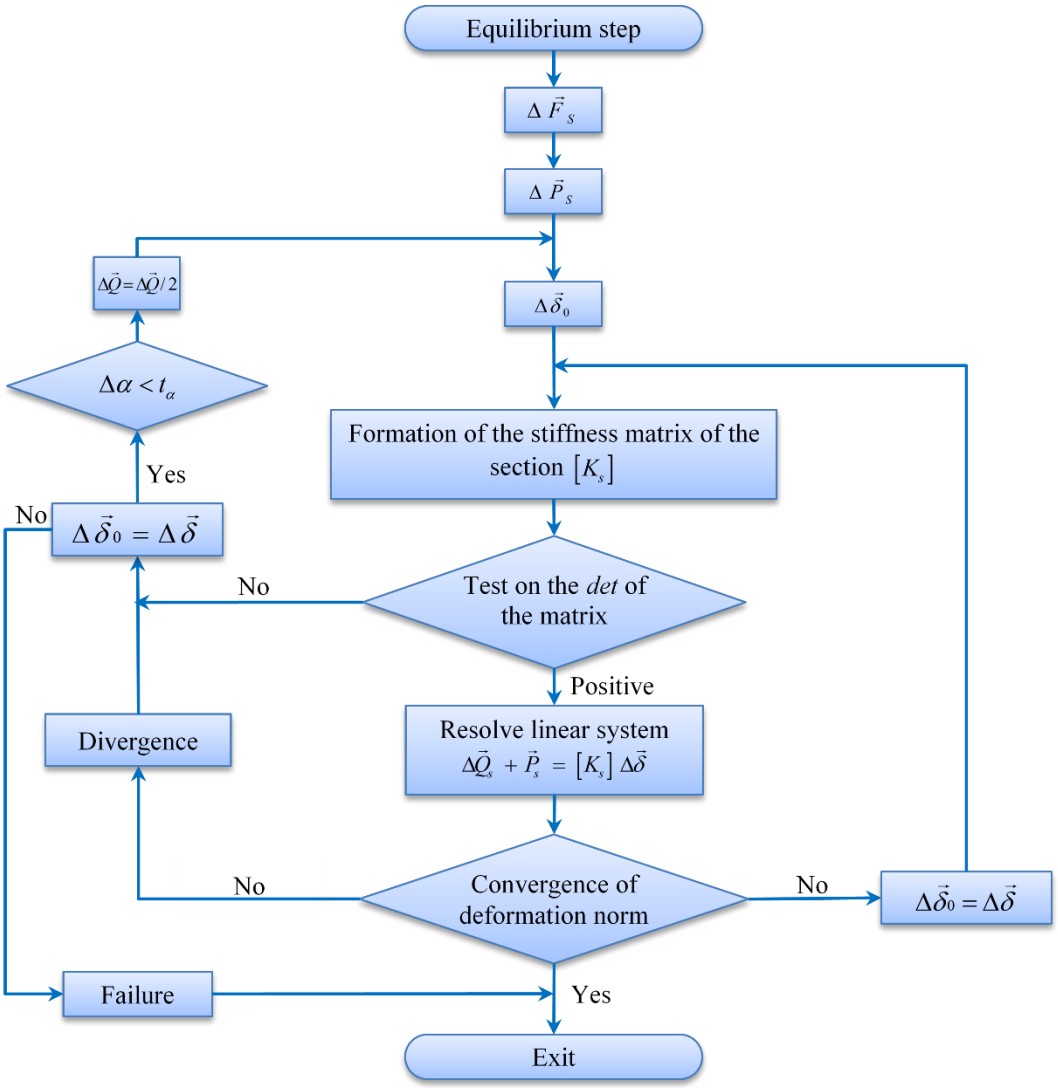

Fig.5 – Simplified organigram of the search for the equilibrium state of a section.

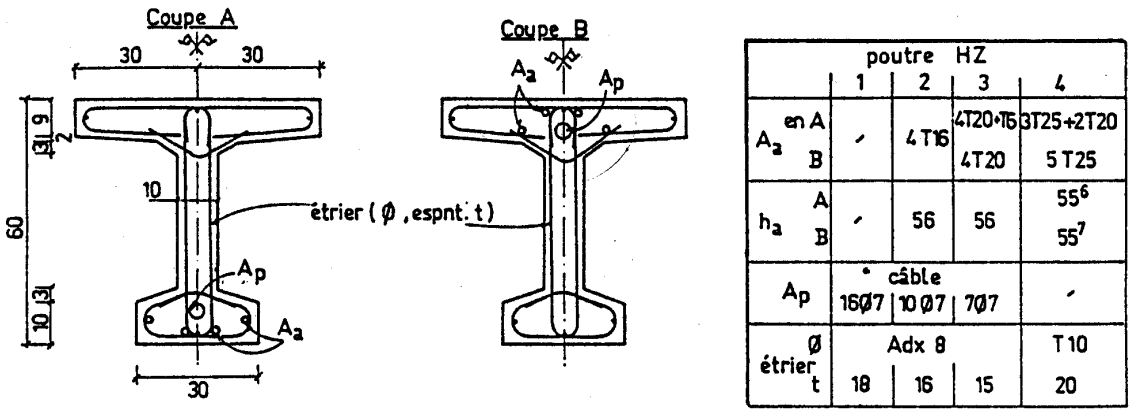

		poutre HZ 1	2	3	4
A_a	en A	″	4 T16	4T20+T16	3T25+2T20
	B			4T20	5 T25
h_a	A	″	56	56	55^6
	B				55^7
Ap	câble	16Ø7	10 Ø7	7Ø7	″
étrier	Ø	Adx 8			T 10
	t	18	16	15	20

Fig. 6 – Dimensions and details of reinforcements for beams HZ [17].

3 Comparison with experimental results

3.1 Simulations of reinforced or prestressed beams

The computing method is used for calculation of four beams HZ tested by Trinh at C.E.B.T.P. [17] with the rates of reinforcement varying from 0 % of prestress (for HZ1) to 100 % of prestress (for HZ4). The length of the beams is 10.40 m, the beams are identical in form and dimensions and made up of two span. The length of each span is 5m. The beams are loaded by two identical loads applied at each mid span. The reinforcement details of the beams are shown on figure 5, and the characteristics of the materials are given in table 1.

Table 1 – Steel and concrete characteristics Trinh [17].

Concrete				Reinforcement			
beam	**f_{cj} *(MPa)***	**f_{tj} *(MPa)***	**E_{ij} *(MPa)***	**steel**	**f_e *(MPa)***	**E_a *(GPa)***	**f_u *(MPa)***
HZ1	39	3.4	35400	ϕ 6	340	206	435
HZ2	33	3.0	31250	HA10	428	198	545
HZ3	34	3.4	32080	HA16	430	213	526
HZ4	32	3.3	32000	HA20	424	195	543
				HA25	450	230	558

The complex arrangement of longitudinal reinforcements for different beams (HZ2, 3, 4) is given by Trinh [17].

The figures 7 to 10 shows the evolution of the beams deflexion at the loading point as function of the applied load for the HZ beams, in the experience, in proposed method and in a non linear calculus with shear stiffness preserve the linear elastic value.

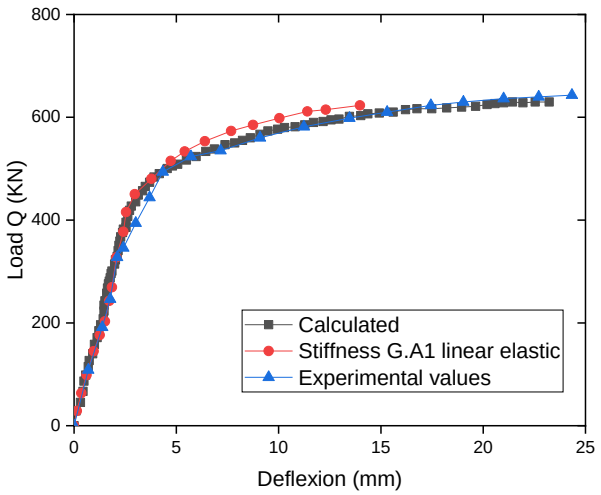

Fig.7 – Load-deflexion curves for beam HZ1.

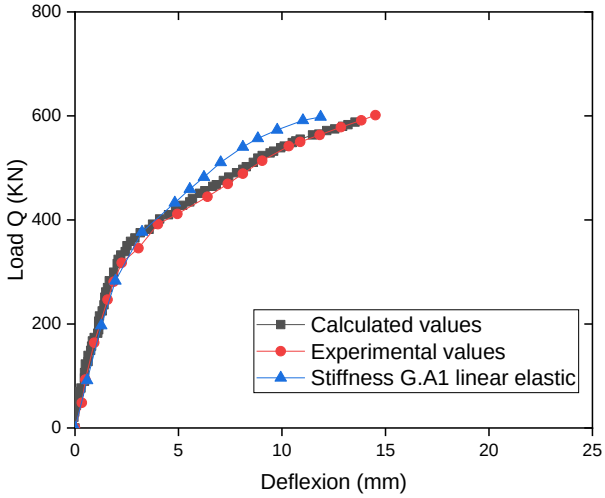

Fig.8 – Load-deflexion curves for beam HZ2.

The predicting results of the model compared with the test results show that, on the one hand, the model predictions are in good agreement with the experimental behaviour in any field of the behaviour (after cracking, post cracking, post steel yielding and fracture of beam), and, on the other hand, the model permits to predict flexural fracture modes (HZ1 and HZ2) and shearing fracture modes (HZ3 and HZ4) for concrete beams with the rate of reinforcement varying from 0 % to 100 % of prestress. The influence of tacking of account of shear-deflexion is visible in figures 9 and 10: it explains the difference of behavior in the case of shearing fracture, in particular in reinforced concrete beam (HZ4).

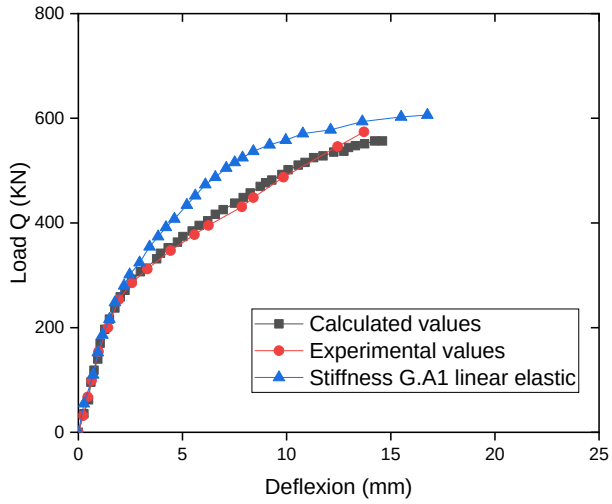

Fig.9 – Load-deflexion curves for beam HZ3.

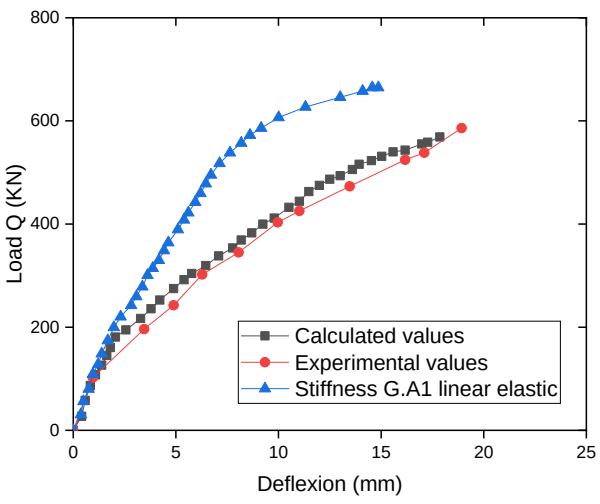

Fig.10 – Load-deflexion curves for beam HZ4.

3.2 Externally prestressed beams

The computing method is used for the calculation of six beams (NM) tested at the CEBTP structural laboratory [11, 18]. The beams are identical in form and dimensions and made up of one span. The length of the span is 6 m. The system loading, the geometrical characteristics, the details of the reinforcement and of the prestress are shown in figure 11. The principal characteristics of the NM-beams are given in Table 2.

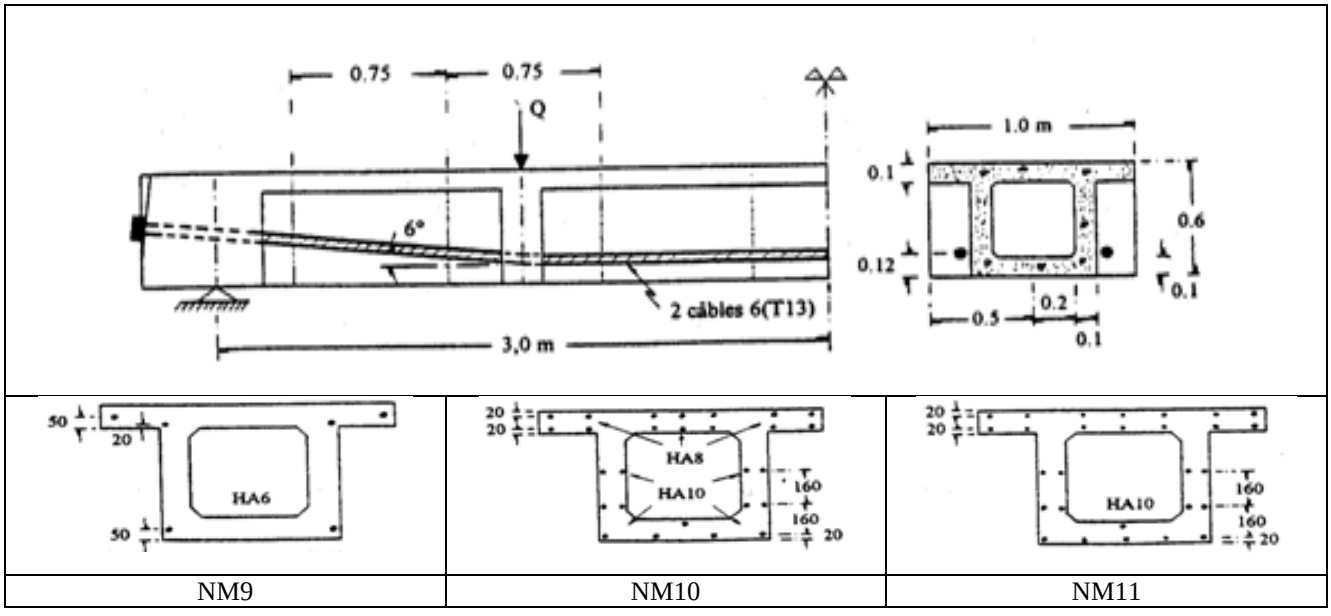

Fig.11 – Geometrical Characteristics and loading system for beams (NM) [11].

Table 2 – Principal characteristics of the NM-Beams.

Beam	Tendon	Reinforcement	Impregnation
NM9	External	W = 0,02%	Wax
NM10	External	W = 0,77%	Cement
NM11	External	W = 0,5%	Wax

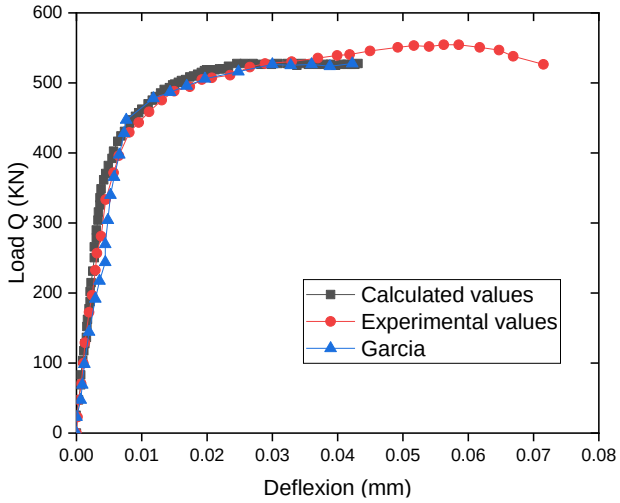

Fig. 12 – Load-deflexion curves for beams (NM9).

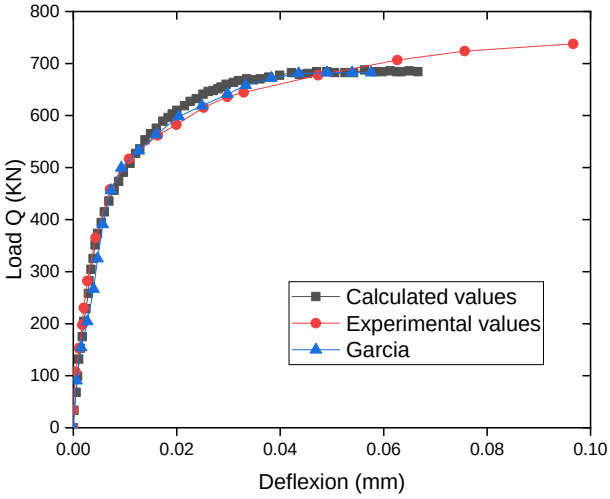

Fig. 13 – Load-deflexion curves for beams (NM10).

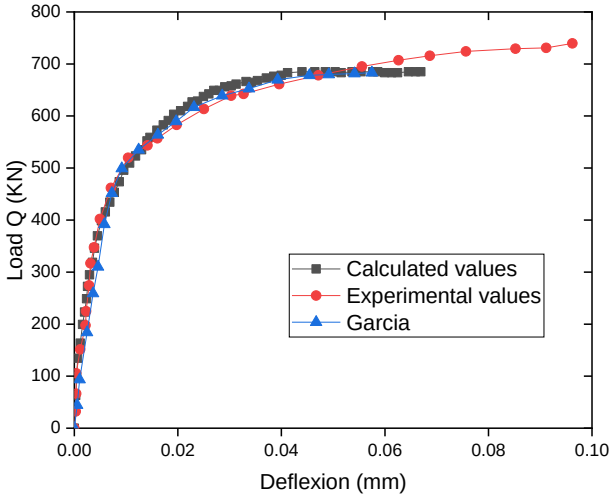

Fig. 14 – Load-deflexion curves for beams (NM11).

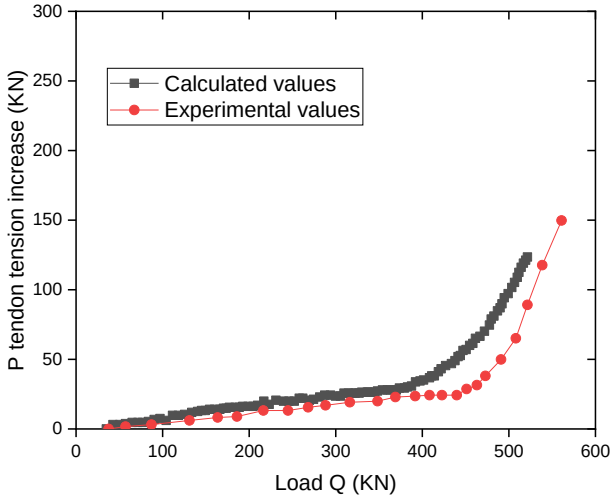

Fig. 15 – Overstress in cable element for beam (NM9).

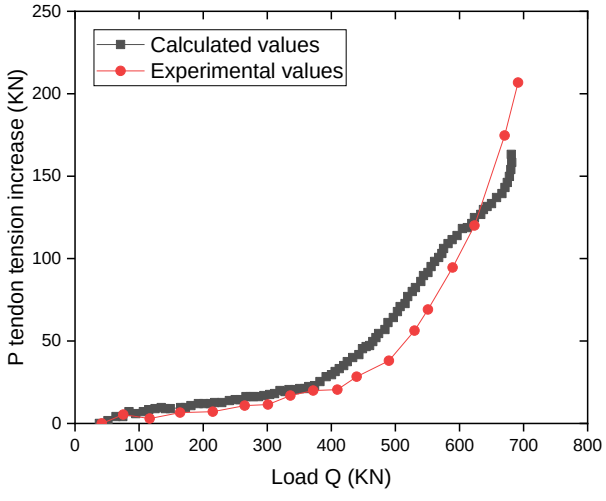

Fig. 16 – Overstress in cable element for beam (NM10)

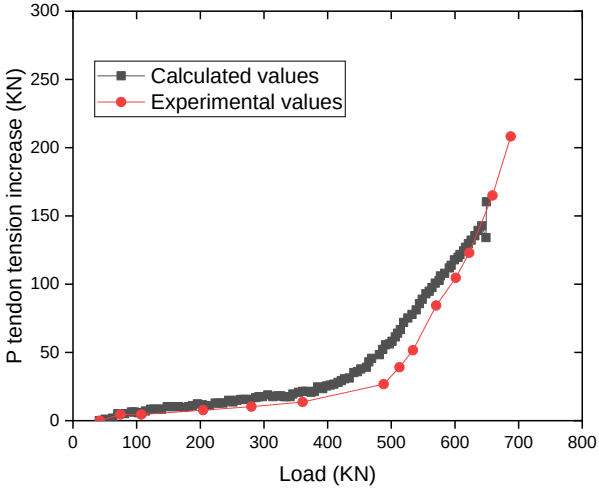

Fig. 17 – Overstress in cable element for beam (NM11).

On figures 12 to 14 the load-deflexion results obtained by the present computing method are compared to these experimental results and also to results obtained by Garcia [19]. The model predictions developed in this work (considering splitting at deviators and varying shear modulus in non linear behaviour) give a good agreement with the experimental behaviour in any field of the behaviour (after cracking, post cracking, post steel yielding and fracture of beam), and up to a value of the deflexion bigger than a limit value obtained by Garcia who considered the shear modulus G to be constant and equal to the shear modulus obtained in linear elasticity. On figures 15 to 20 overstress in cable elements and slipping of tendons at deviators obtained by the present computing method are compared to the experimental results. It may be seen that the model exhibits a good agreement for the deferent's stages of the behaviour [16, 20-26].

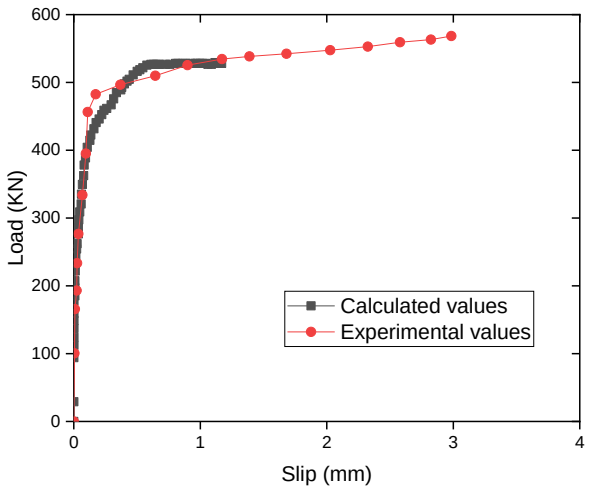

Fig. 18 – Slip of tendon at deviators beam (NM9)

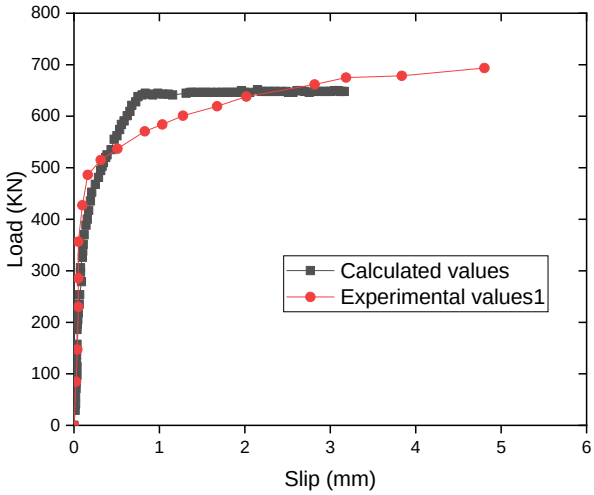

Fig. 19 – Slip of tendon at deviators beam (NM10).

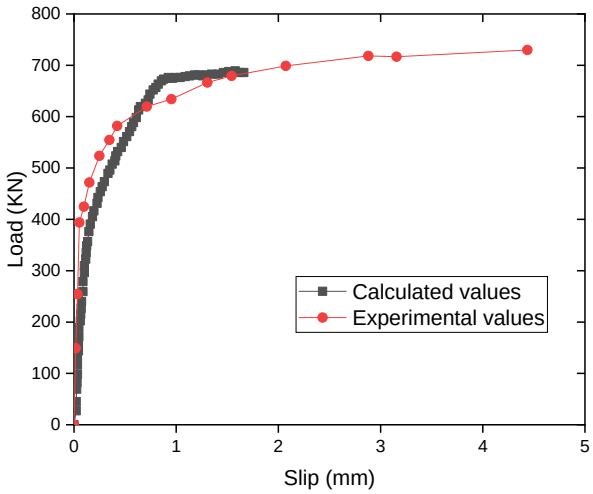

Fig. 20 – Slip of tendon at deviators for the beam (NM11)

4 Conclusion and perspectives

We presented a model based on the strip-analysis of the sections and on an iterative technique to find the angle of inclination of the diagonal compression using stress and strain Mohr's circles properties to solve a complex system of equations for the determination of shear stresses distribution and of the distortion distribution. On the one hand, this model is able to predict the behaviour of beams with sections having unusual shapes or reinforcing details, loaded in combined

bending, axial load and shear. On the second hand, it permits to predict flexural fracture mode and shearing fracture mode (see HZ4) for concrete beams with the detail of reinforcements varying from 0 % to 100 % of prestress. Furthermore, this model permits to follow the behaviour of beams until very high values of the beam deflexion.

In the case of externally prestress (NM), this model permits to predict the behaviour of beams up to very high values of the beam deflexion, to calculate the tendons slipping at the deviators and to estimate the overstress in the tendons at each stage of loading. Indeed, the fracture mode is correctly predicted for the Beams NM. The shear stiffness seem that draw near the elastic linear shear stiffness after concrete cracking, before this, it's proposed evaluation permit to follow the beams behaviour until a higher value of the deflexion comparatively to the calculation with the linear elastic shear stiffness. We can see equally that the value of the fracture load calculated give very good agreement with the experimental value of this parameter. The tendon slipping for each beam NM seems to be evaluated correctly after concrete cracking and permit to follow before this the tendon slipping equally until a relatively high value for the slip. We can finally see that the evaluated overstress in the tendons give a very good agreement with the experimental values for each stage of the loading.

For better estimation of the final slip at the total failure of the beams with external prestressing, we recommend new study with refinement of the gridding and choose another numerical resolution method (example; stepwise incremental resolution of loading).We could also point out the case of the taking into account of several cables which slide differently, the effect of the torsion and also taking into account of the presence of fiber- reinforced concrete [2, 3] in the case of tensioned diagonal elements (truss beams).Finally, the proposed numerical procedure makes easy the possibility of introduction other material's behaviour laws.

A_j: section of the bare i

b_i : base width of the layer i

y_{aj} : coordinate of the bare j

E_a : steel young modulus

E_p : prestress young modulus

f : the curved friction coefficient

f_{ei} : yielding stress of reinforcement

f_{cj} : concrete compressive strength

f_{ct} : concrete tensile strength

h_i : height of the layer i

k'_b : Sargin law parameter

k_b : Sargin law parameter

L : the beam element length

L_0 : the initial element length

M: moment

M1: moment in the section 1

M2 : moment in the section 2

N: normal load

N1: normal load in the section 1

N2: normal load in the section 2

V: shear

ϕ_e : the cable diameter,

ΔV : shear force increase.

e : élément length increase

$\Delta\vec{g}$: the vector of slippings,

u : translation between the local system and intermediate system in the x_0 direction

v : translation between the local system and intermediate system in the y_0 direction

θ : nodal rotation in the intrinsic system

A_d : factor taking into account the bond of the cable element (d) at the deviator.

$\Delta\vec{U}$ the increase of the nodal displacements in the global system coordinates

R : the global stiffness matrix of the structure,

$\Delta\vec{P}$: the global initial prestress-load cable element vector in the global system coordinates

$\Delta\vec{Q}$: the global external loads increase vector in the global system coordinates

$\Delta\vec{F}_u$: nodal loads increase in the intermediate system coordinates

B : transformation matrix from intrinsic system to intermediate system coordinates

$\Delta\vec{S}_u$: the nodal displacements in the intermediate system coordinates

K_n : the element stiffness matrix in the intrinsic system coordinates

$\Delta\vec{F}_n$: nodal loads increase in the intrinsic system c

$\Delta\vec{S}_n$: the nodal displacements in the intrinsic system

$\Delta\vec{P}_n$: the initial prestress-load cable element vector in the intrinsic system coordinates

$\Delta\vec{F}_L$: nodal loads increase in the local system

$\Delta\vec{S}_L$: the nodal displacements in the local system

$\Delta\vec{P}_L$: the initial prestress-load cable element vector in the local system coordinates

$\mathbf{T_0}$ **:** translation matrix between intermediate system and local system coordinates

$\Delta\vec{F}_G$: nodal loads in the global system coordinates

$\Delta\vec{S}_G$: the nodal displacements in the global system

$\Delta\vec{P}_G$: the initial prestress-load cable element vector in the global system coordinates

$\mathbf{T_G}$ **:** rotation matrix du local system to global system

f_{ep} : stress fracture of prestressing steel bars

σ_r : compressive stress fracture of concrete

ΔW_e : the external shear work,
ΔW_i : the work internal shear
σ : Stresses
ΔN : axial load increase;
ΔM : bending moment increase;
G : the rigidity matrix of slipping
ε : strain
ε_{cu}: ultimate concrete strain
$\varepsilon_{p:}$ prestress cable strain
ε_{ct} : concrete cracking strain
ε_{rt} : tensile concrete ultimate strain
$\Delta\delta u$: the axial strain increase
$\Delta\delta w$: the curvature increase
$\Delta\gamma_{moy}$: the mean distortion increase.
K_s : the section stiffness matrix
L_k : the length of the deviator *k*
$\Delta\tau_i$: the shear stress increase
σ_p : stress of the prestress cable
σ_e : yielding stress of the reinforcement
σ_{ep} : yielding stress of the prestress cable
$\Delta\varepsilon_g$: the cable element axial strain increase
F_d : the tension in the cable elements
φ *:* the straight friction coefficient ,
$\Delta\varepsilon_p$: pre deformation of the prestress steel
r : the radius of curvature of the cable at the deviator *k*.
θ_d : the deviation angles of cable elements (*d*)
$\vec{F}_k$: the tensile forces in the cable elements
ρ_{yi} : transverse reinforcement percentage of the layer i
ε_e : yielding strain of the reinforcement
ε_u ultimate strain of the reinforcement
ε_0: concrete strain corresponding to f_{cj}
$\Delta\vec{F}_S$: the vector of exterior loads increase
β_d :coefficient of the sense of the slipping
$\Delta\vec{P}_S$: the internal tendon initial prestress-action
s : distance between the section 1 and the section 2
g_d : the absolute value of the slipping
$\Delta\vec{P}_u$: the initial prestress-load cable element vector in the intermediate system coordinates

REFERENCES

[1]- N. Ariyawardena, A. Ghali, Prestressing with Unbonded Internal or External Tendons: Analysis and Computer Model. J. Struct. Eng., 128(12) (2002) 1493-1501. doi:10.1061/(ASCE)0733-9445(2002)128:12(1493).

[2]- Y. Bouafia, M.S. Kachi, D. Atlaoui, S. Djebali, Study of Mechanical Behavior of Concrete in Direct Tensile Fiber Chips. Appl. Mech. Mater., 146 (2012) 64-73. doi:10.4028/www.scientific.net/AMM.146.64.

[3]- B. Mansour, Model of Behavior at Pulling of the Reinforced Concrete of Waved Fibers. Bulletin of Applied Mechanics, 6(21) (2010) 6-11.

[4]- A. Dall'Asta, L. Dezi, Nonlinear Behavior of Externally Prestressed Composite Beams: Analytical Model. J. Struct. Eng., 124(5) (1998) 588-597. doi:10.1061/(ASCE)0733-9445(1998)124:5(588).

[5]- A. Grelat, Comportement non linéaire et stabilité des ossatures en béton armé. Annales de l'Institut technique du bâtiment et des travaux publics, (1978).

[6]- M.S. Kachi. Modélisation du comportement jusqu'à rupture des poutres à précontrainte extérieur. Thèse de doctorat. Université Mouloud Mammeri de Tizi-Ouzou, 2006.

[7]- M.S. Kachi, B. Fouré, Y. Bouafia, P. Muller, L'effort trenchant dans la modélisation du comportement jusqu' à rupture des pouters en béton armé et précontraint. Revue Européenne de Génie Civil, 10(10) (2006) 1235-1264. doi:10.1080/17747120.2006.9692914.

[8]- T. Kiang-Hwee, N. Chee-Khoon, Effects of Deviators and Tendon Configuration on Behavior of Externally Prestressed Beams. ACI Structural Journal, 94(1) (1997). doi:10.14359/456.

[9]- E.K.G.L.F. Michael, C.E.-H. Kamal, Finite Element Analysis of Externally Post-Tensioned Segmental Box Girder construction. ACI Symposium Publication, 120. doi:10.14359/2859.

[10]- O. Nait-Rabah. Simulation numérique du comportement non-linéaire des ossatures spatiales: application aux structures en béton armé, en béton précontraint et mixtes. Thèse de doctorat. Châtenay-Malabry, Ecole centrale de Paris, 1990.

[11]- B. Fouré, P. De Rezende Martins, L.H. Hoang. Problèmes de sécurité à rupture et de modélisation du comportement

des poutres en béton à précontrainte extérieure. in Annales de l'Institut technique du bâtiment et des travaux publics. (1991.

[12]- C.K. Ng, K.H. Tan, Flexural behaviour of externally prestressed beams. Part I: Analytical model. Eng. Struct., 28(4) (2006) 609-621. doi:10.1016/j.engstruct.2005.09.015.

[13]- T. Kiang-Hwee, A.T. Robert, Shear Deficiency in Reinforced Concrete Continuous Beams Strengthened with External Tendons. ACI Structural Journal, 100(5). doi:10.14359/12797.

[14]- T.-j. Lou, Y.-q. Xiang, Finite element modeling of concrete beams prestressed with external tendons. Eng. Struct., 28(14) (2006) 1919-1926. doi:10.1016/j.engstruct.2006.03.020.

[15]- B. Règles, modifiées 99 (Règles techniques de conception et de calcul des ouvrages et constructions en béton préconrtaint suivant la méthode des états limites), fascicule n 62 titre 1er section II du CCTG applicable aux marchés publics de travaux. JO du, 16 (1999).

[16]- A. Adjrad, Y. Bouafia, M.S. Kachi, H. Dumontet, Non-linear modelling of three dimensional structures taking into account shear deformation. International Journal of Engineering and Technology, 6(4) (2014) 290.

[17]- J. Trinh. Précontrainte partielle: essais de poutres continues. in Annales de l'Institut technique du bâtiment et des travaux publics. (1995), 1-32.

[18]- B. Fouré, P. Rezende-Martins, Comportement en flexion jusqu'à rupture des poutres à précontrainte extérieure. La Technique Française du Béton Précontrainte–AFPC, XI Congrès de la FIP, Hambourg, (1990).

[19]- J. Garcia-Vargas. Effect of external tendon slipping at deviator on beam behavior. in Proceedings of the Workshop on Behavior of External Prestressing in Structures, France. (1993), 227-237.

[20]- M. Virlogeux, A. M'Rad. Flexural behaviour of externally prestressed structures for ultimate loads. in Proceedings of the Workshop on Behaviour of External Prestressing in Structures, Saint-Rémy–les-Chevreuses, France, June. (1993.

[21]- M. Virlogeux, External pretressing: from construction history to modern technique and technology, External prestressing in bridges, ACI, SP-120, Éd. Antoine Naamane and John Breen, (1990).

[22]- A. Zona, L. Ragni, A. Dall'Asta, Finite element formulation for geometric and material nonlinear analysis of beams prestressed with external slipping tendons. Finite Elements in Analysis and Design, 44(15) (2008) 910-919. doi:10.1016/j.finel.2008.06.005.

[23]- A. Adjrad, Y. Bouafia, M.S. Kachi, H. Dumontet, Modeling of Externally Prestressed Beams until Fracture in Non Linear Elasticity. Appl. Mech. Mater., 749 (2015) 379-385. doi:10.4028/www.scientific.net/AMM.749.379.

[24]- A. Adjrad, Y. Bouafia, M.S. Kachi, F. Ghazi, Prediction of the Rupture of Circular Sections of Reinforced Concrete and Fiber Reinforced Concrete. Int. J. Concrete Struct. Mater. 10(3) (2016) 373-381. doi:10.1007/s40069-016-0137-8.

[25]- F. Iguetoulene. Modélisation non linéaire des structures triangulées. Doctoral Thesis, Université Mouloud Mammeri, 2011.

[26]- D. Bouchafa, M.S. KACHI, Y. Bouafia, K. BENYAHI, S. Barboura, Numerical simulation and reliability of behaviour until the rupture of reinforced concrete spacial structure members with circular cross section. J. Mater. Eng. Struct. 8(1) (2021) 61-82.